

Quantum Computing, Metrology, and Imaging

Hwang Lee, Pavel Lougovski, and Jonathan P. Dowling

Department of Physics and Astronomy
Hearne Institute for Theoretical Physics
Louisiana State University, Baton Rouge, LA 70803-4001

ABSTRACT

Information science is entering into a new era in which certain subtleties of quantum mechanics enables large enhancements in computational efficiency and communication security. Naturally, precise control of quantum systems required for the implementation of quantum information processing protocols implies potential breakthroughs in other sciences and technologies. We discuss recent developments in quantum control in optical systems and their applications in metrology and imaging.

Keywords: Quantum computing, quantum entanglement, optical interferometers, High NOON states, Heisenberg limit

1. INTRODUCTION

A new concept of quantum computation has been developed in recent years. The basic unit of a quantum computer is a quantum mechanical two-level system (qubit) that can be in coherent superpositions of the logical values 0 and 1, as opposed to classical bits that represent either the values 0 or 1. Moreover, qubits can possess mutually tied properties while separated in space, so-called quantum entanglement. The implementation of computations is carried out by unitary transformations, which consist of the individual quantum logic gates. The utilization of superposition and entanglement leads to a high degree of parallelism, which makes the speed of certain types of computation exponentially faster than the classical counterpart.¹

It has been known for a while that quantum entanglement has the potential to revolutionize the entire field of interferometry by providing many orders of magnitude improvement in interferometer sensitivity. In particular, without nonlocal entanglement, a generic classical interferometer has a statistical-sampling shot-noise limited sensitivity. However, if carefully prepared quantum correlations are engineered between the particles, then the interferometer sensitivity improves beyond the shot-noise limit.

A few years ago we introduced the Quantum Rosetta Stone by addressing the formal equivalence between a generic quantum logic gate, a Ramsey-type atomic clock, an optical Mach-Zehnder interferometer.² The Quantum Rosetta Stone instigated transparent communication between the workers in these different areas of research, allowing them to adapt the techniques developed in the other areas to their own research—greatly advancing all three fields. In particular, we focus on the recent developments in optical implementations of quantum computing and address their utilization in quantum metrology and imaging for general audience.

2. OPTICAL QUANTUM COMPUTING

In optical approach to quantum computation, qubits are usually represented by the state of polarization of a single photon. The main difficulty lies in the fact that the necessary two-qubit logic gates need a nonlinear interaction between the two photons and the efficiency of this nonlinear interaction is typically very tiny at the single-photon level. This obstacle, however, can be avoided by making corrections to the output of the logic devices based on the results of single-photon detectors. In this section we describe the basic one-qubit operations, non-deterministic two-qubit gates, near-deterministic two-qubit gates, and certain issues related to their implementations.

¹SPIE's International Symposium on Fluctuations and Noise, Austin, TX (May, 2005).

2.1. One-qubit gates

The one-qubit gates necessary for an arbitrary operation are any two of x-rotation, y-rotation, and z-rotation, and a phase gate. The x-rotation, $R_x(\theta)$ is formally written as

$$\begin{aligned} R_x(\theta) &= e^{i\sigma_x \frac{\theta}{2}} = \cos \frac{\theta}{2} + i\sigma_x \sin \frac{\theta}{2} = \cos \frac{\theta}{2} + i \begin{pmatrix} 0 & 1 \\ 1 & 0 \end{pmatrix} \sin \frac{\theta}{2} \\ &= \begin{pmatrix} \cos \frac{\theta}{2} & i \sin \frac{\theta}{2} \\ i \sin \frac{\theta}{2} & \cos \frac{\theta}{2} \end{pmatrix}. \end{aligned} \quad (1)$$

Similarly, y-rotation and z-rotation read

$$\begin{aligned} R_y(\theta) &= e^{i\sigma_y \frac{\theta}{2}} = \cos \frac{\theta}{2} + i\sigma_y \sin \frac{\theta}{2} = \cos \frac{\theta}{2} + i \begin{pmatrix} 0 & -i \\ i & 0 \end{pmatrix} \sin \frac{\theta}{2} \\ &= \begin{pmatrix} \cos \frac{\theta}{2} & \sin \frac{\theta}{2} \\ -\sin \frac{\theta}{2} & \cos \frac{\theta}{2} \end{pmatrix}, \end{aligned} \quad (2)$$

$$\begin{aligned} R_z(\theta) &= e^{i\sigma_z \frac{\theta}{2}} = \cos \frac{\theta}{2} + i\sigma_z \sin \frac{\theta}{2} = \cos \frac{\theta}{2} + i \begin{pmatrix} 1 & 0 \\ 0 & -1 \end{pmatrix} \sin \frac{\theta}{2} \\ &= \begin{pmatrix} e^{i\frac{\theta}{2}} & 0 \\ 0 & e^{-i\frac{\theta}{2}} \end{pmatrix}. \end{aligned} \quad (3)$$

Finally, the phase gate is given by

$$Ph(\theta) = \begin{pmatrix} e^{i\theta} & 0 \\ 0 & e^{-i\theta} \end{pmatrix}. \quad (4)$$

Let us suppose now the qubit is encoded in the polarization degrees of freedom of a single photon so that the logical qubit is given by

$$|0\rangle \equiv |H\rangle, \quad |1\rangle \equiv |V\rangle. \quad (5)$$

(i) Phase gate

Then, the z-rotation, for example, can be achieved by a waveplate and phase shifters. The wave plate is a doubly refracting (birefringent) transparent crystal where the index of refraction is larger for the slow axis than the one for the fast axis. Let us assume that the slow axis is vertical direction and the fast is the horizontal direction. After propagating by a distance d , the vertically polarized light acquires a phase shift of $\exp[in_1 \frac{2\pi}{\lambda} d]$, and similarly, the horizontally polarized light acquires $\exp[in_2 \frac{2\pi}{\lambda} d]$ ($n_1 > n_2$). The relative phase shift acquired by the vertically polarized light is then

$$|V\rangle \Rightarrow e^{i(n_1 - n_2) \frac{\lambda}{2} d} |V\rangle \equiv e^{i\phi} |V\rangle \quad (6)$$

If we choose the thickness of the crystal such that

$$d = \frac{\lambda/4}{n_1 - n_2}, \quad (7)$$

then the relative phase shift $\phi = \pi/2$. This corresponds to the *quarter wave plate* as one can write

$$|H\rangle + |V\rangle \Rightarrow |H\rangle + e^{i\pi/2}|V\rangle \quad (9)$$

Using the convention for left and right circularly polarized light,

$$\hat{e}_- = \frac{1}{\sqrt{2}}(\hat{e}_1 + i\hat{e}_2), \quad \hat{e}_+ = \frac{1}{\sqrt{2}}(\hat{e}_1 - i\hat{e}_2) \quad (10)$$

A linearly polarized light ($|H\rangle + |V\rangle$) becomes an left circularly polarized light. In general, an arbitrary phase angle, ϕ can be made by choosing the thickness d as

$$d = \frac{\lambda}{n_1 - n_2} \frac{\phi}{2\pi} \quad (11)$$

On the other hand, the overall phase factor also depends on the value of ϕ such that

$$\begin{aligned} e^{in_2 \frac{2\pi}{\lambda} d} &= e^{in_2 \frac{2\pi}{\lambda} \frac{\lambda}{2\pi} \frac{\phi}{n_1 - n_2}} \\ &= e^{i \frac{n_2}{n_1 - n_2} \phi}, \end{aligned} \quad (12)$$

(ii) z-rotation

Now for the z-rotation, we have

$$\begin{aligned} R_z(\theta)[|0\rangle + |1\rangle] &= e^{i\frac{\theta}{2}}|0\rangle + e^{-i\frac{\theta}{2}}|1\rangle \\ &= e^{i\frac{\theta}{2}}[|0\rangle + e^{-i\theta}|1\rangle] \end{aligned} \quad (13)$$

One can have this operation with a wave plate by taking $\phi = -\theta$. Then, the overall phase factor of Eq.(12) becomes

$$e^{i \frac{n_2}{n_1 - n_2} \phi} = e^{-i \frac{n_2}{n_1 - n_2} \theta} \equiv e^{-ir\theta} \quad (14)$$

where we defined $r = \frac{n_2}{n_1 - n_2}$. In order to match the overall phase factor of the z-rotation ($e^{i\frac{\theta}{2}}$), we need to have a phase shifter such that

$$e^{i\phi'} e^{-ir\theta} = e^{i\frac{\theta}{2}}, \quad (15)$$

yielding

$$\phi' = \frac{\theta}{2}(1 + 2r) = \frac{\theta}{2} \frac{n_1 + n_2}{n_1 - n_2} \equiv s\theta \quad (16)$$

Therefore, the z-rotation is made by a wave plate of $-\theta$ and a phase shifter of $s\theta$, where $s = [(n_1 + n_2)/2(n_1 - n_2)]$. Symbolically, we may write this relation as

$$R_z(\theta) := \text{PS}(s\theta)\text{WP}(-\theta) \quad (17)$$

(iii) x-rotation

Now suppose the wave plate we described above is rotated around the propagation axis by an amount of α . Then the operation by the wave plate can be given as

$$\begin{aligned} \text{WP}(\phi, \alpha = 0) &= e^{ir\phi} \begin{pmatrix} 1 & 0 \\ 0 & e^{i\phi} \end{pmatrix}, \\ \text{WP}(\phi, \alpha) &= e^{ir\phi} \begin{pmatrix} \cos \alpha & -\sin \alpha \\ \sin \alpha & \cos \alpha \end{pmatrix} \begin{pmatrix} 1 & 0 \\ 0 & e^{i\phi} \end{pmatrix} \begin{pmatrix} \cos \alpha & \sin \alpha \\ -\sin \alpha & \cos \alpha \end{pmatrix} \\ &= e^{ir\phi} \begin{pmatrix} \cos^2 \alpha + e^{i\phi} \sin^2 \alpha & \cos \alpha \sin \alpha (1 - e^{i\phi}) \\ \cos \alpha \sin \alpha (1 - e^{i\phi}) & \sin^2 \alpha + e^{i\phi} \cos^2 \alpha \end{pmatrix}. \end{aligned} \quad (18)$$

If we set the rotation angle α equal to $\pi/4$, we obtain

$$\text{WP}(\phi, \alpha = \pi/4) = \frac{e^{ir\phi}}{2} \begin{pmatrix} 1 + e^{i\phi} & 1 - e^{i\phi} \\ 1 - e^{i\phi} & 1 + e^{i\phi} \end{pmatrix}. \quad (19)$$

We can see that the x-rotation $R_x(\theta)$ given in Eq.(1), can be achieved by setting $\phi = -\theta$ as

$$\text{WP}(\phi = -\theta, \alpha = \pi/4) = e^{-ir\theta} e^{-i\frac{\theta}{2}} \begin{pmatrix} \cos \frac{\theta}{2} & i \sin \frac{\theta}{2} \\ i \sin \frac{\theta}{2} & \cos \frac{\theta}{2} \end{pmatrix}. \quad (20)$$

Similarly to the case of $R_z(\theta)$, we compensate the overall phase factor by a phase shifter of $e^{is\theta}$ and then the x-rotation is given by

$$R_x(\theta) := \text{PS}(s\theta)\text{WP}(-\theta, \alpha = \pi/4). \quad (21)$$

One can then construct the y-rotation by using

$$R_y(\theta) = R_z(-\frac{\pi}{2})R_x(\theta)R_z(\frac{\pi}{2}) \quad (22)$$

(iv) Hadamard gate

Having the x-rotation, z-rotation, and the phase gate, it is now sufficient to build any arbitrary one qubit gate. For example, the Hadamard gate, one of the most frequently used one-qubit gates in the literature, can be build as follows.

$$\begin{aligned} H &= \frac{1}{\sqrt{2}} \begin{pmatrix} 1 & 1 \\ 1 & -1 \end{pmatrix} \\ &= \text{Ph}(-\frac{\pi}{2})R_z(\pi)R_y(\frac{\pi}{2}) \\ &= \text{Ph}(-\frac{\pi}{2})R_z(\pi)R_z(-\frac{\pi}{2})R_x(\frac{\pi}{2})R_z(\frac{\pi}{2}) \\ &= \text{Ph}(-\frac{\pi}{2})R_z(\frac{\pi}{2})R_x(\frac{\pi}{2})R_z(\frac{\pi}{2}) \end{aligned} \quad (23)$$

2.2. Two-qubit gates

A typical two-qubit gate, controlled-NOT (CNOT) is represented as follows:

$$\begin{aligned}
|0\rangle_L|0\rangle_L &\rightarrow |0\rangle_L|0\rangle_L \\
|0\rangle_L|1\rangle_L &\rightarrow |0\rangle_L|1\rangle_L \\
|1\rangle_L|0\rangle_L &\rightarrow |1\rangle_L|1\rangle_L \\
|1\rangle_L|1\rangle_L &\rightarrow |1\rangle_L|0\rangle_L,
\end{aligned} \tag{24}$$

where the second qubit (target) flips when the first qubit (control) has in the logical value 1. The CNOT gate plays an important role in that any n-qubit gates can be decomposed into the CNOT gates and one-qubit gates and thus form a universal set of gates.

To physics community, however, the conditional sign flip is perhaps more familiar. The transformation by the conditional sign-flip gate is written as

$$\begin{aligned}
|0\rangle_L|0\rangle_L &\rightarrow |0\rangle_L|0\rangle_L \\
|0\rangle_L|1\rangle_L &\rightarrow |0\rangle_L|1\rangle_L \\
|1\rangle_L|0\rangle_L &\rightarrow |1\rangle_L|0\rangle_L \\
|1\rangle_L|1\rangle_L &\rightarrow -|1\rangle_L|1\rangle_L.
\end{aligned} \tag{25}$$

The CNOT gate is then simply constructed by using the conditional sign flip and two one-qubit gates (e.g., Hadamard on the target, followed by the conditional sign flip and another Hadamard on the target). Note that the CNOT is the controlled σ_x operation whereas the C-Z gate is the controlled σ_z operation

The optical Kerr nonlinearity was first considered for such a conditional sign flip. The interaction caused by the Kerr nonlinearity can be described by a Hamiltonian³

$$\mathcal{H}_{\text{Kerr}} = \hbar\kappa\hat{a}^\dagger\hat{a}\hat{b}^\dagger\hat{b}, \tag{26}$$

where κ is a coupling constant depending on the third-order nonlinear susceptibility, and \hat{a}^\dagger , \hat{b}^\dagger and \hat{a} , \hat{b} are the creation and annihilation operators for two optical modes. One convenient choice of the logical qubit can then be represented by the two modes containing a single photon, denoted as

$$\begin{aligned}
|0\rangle_L &= |0\rangle_l |1\rangle_k \\
|1\rangle_L &= |1\rangle_l |0\rangle_k,
\end{aligned} \tag{27}$$

where l, k represent the relevant modes, and we have used the notation $|\cdot\rangle_L$ for a logical qubit, in order to distinguish it from the photon-number states $|\cdot\rangle_k$. The conversion between this so-called dual rail qubit and the polarization qubit can be simply made by polarizing beam splitters.

Now let us assign mode 1,2 for the control qubit, and 3,4 for the target qubit. Suppose now only the modes 2,4 are coupled under the interaction given by Eq.(26). For a given interaction time τ , the transformation can be written as

$$\begin{aligned}
|0\rangle_L|0\rangle_L &\rightarrow |0\rangle_L|0\rangle_L \\
|0\rangle_L|1\rangle_L &\rightarrow |0\rangle_L|1\rangle_L \\
|1\rangle_L|0\rangle_L &\rightarrow |1\rangle_L|0\rangle_L \\
|1\rangle_L|1\rangle_L &\rightarrow e^{i\varphi}|1\rangle_L|1\rangle_L,
\end{aligned} \tag{28}$$

where $\varphi \equiv \kappa n_a n_b \tau$ and $n_a = \langle \hat{a}^\dagger \hat{a} \rangle$, $n_b = \langle \hat{b}^\dagger \hat{b} \rangle$. This operation yields a conditional phase shift. When $\varphi = \pi$, we have the two two-qubit gate called the conditional sign-flip gate. In order to have $\varphi \sim \pi$ at the single-photon level, however, a huge third-order nonlinear coupling is required.⁴ However, this barrier can be circumvented by quantum teleportation technique in one hand, and effective nonlinearities produced by projective measurements in the other.⁵

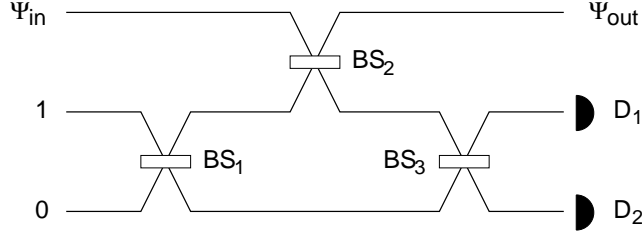


Figure 1. Nonlinear sign gate: The input state of $|\Psi_{\text{in}}\rangle = \alpha|0\rangle + \beta|1\rangle + \gamma|2\rangle$ transforms to $|\Psi_{\text{out}}\rangle = \alpha|0\rangle + \beta|1\rangle - \gamma|2\rangle$ upon detection of one photon at D_1 and non-detection at D_2 .

2.3. Nonlinear sign gate

Together with quantum teleportation the nonlinear sign (NS) gate serves the basic element in the architecture of linear optics quantum computation. The NS gate applies to photon number state consists of zero, one and two photons as is defined by

$$\alpha|0\rangle + \beta|1\rangle + \gamma|2\rangle \rightarrow \alpha|0\rangle + \beta|1\rangle - \gamma|2\rangle. \quad (29)$$

The NS gate can be implemented non-deterministically by three beam splitters, two photo-detectors, and one ancilla photon as depicted in Fig.1. Conditioned upon a specific detector outcome, we can have the desired output state with probability of 1/4. The gate operation succeeds only once in four times on average. But, the merit is that we know we it was successful whenever it was successful.

Now we need to fix the reflection coefficients of the three beam splitters utilized in the nonlinear sign gate. Taking \hat{a} and \hat{b} as the input modes, the output modes can be found as

$$\begin{pmatrix} \hat{a}' \\ \hat{b}' \end{pmatrix} = \begin{pmatrix} r & t \\ t & r \end{pmatrix} \begin{pmatrix} \hat{a} \\ \hat{b} \end{pmatrix} \quad (30)$$

where for lossless beam splitters the reflection coefficient r and the transmission coefficient t need to satisfy $|r|^2 + |t|^2 = 1$, and $rt^* + tr^* = 0$. We may define the beam splitter as

$$\text{BS}(\theta, \phi) := \begin{pmatrix} \cos \theta & e^{i\phi} \sin \theta \\ e^{i\phi} \sin \theta & \cos \theta, \end{pmatrix} \quad (31)$$

and the following set of beam splitters can to perform the desired operation⁶:

$$\text{BS}_1 = \text{BS}_3 := \begin{pmatrix} \sqrt{\eta} & \sqrt{1-\eta} \\ \sqrt{1-\eta} & -\sqrt{\eta} \end{pmatrix}, \quad \eta = \frac{1}{(4-2\sqrt{2})} \approx 0.854 \quad (32)$$

$$\text{BS}_2 := \begin{pmatrix} -\sqrt{\eta_2} & \sqrt{1-\eta_2} \\ \sqrt{1-\eta_2} & \sqrt{\eta_2} \end{pmatrix}, \quad \eta_2 = (\sqrt{2}-1)^2 \approx 0.172 \quad (33)$$

These beam splitters are phase asymmetric, which can be made by ordinary beam splitters with an additional phase shifters so that we have

$$\text{BS}_1 = \text{BS}_3 := \begin{pmatrix} 1 & 0 \\ 0 & i \end{pmatrix} \begin{pmatrix} \sqrt{\eta} & -i\sqrt{1-\eta} \\ -i\sqrt{1-\eta} & \sqrt{\eta} \end{pmatrix} \begin{pmatrix} 1 & 0 \\ 0 & i \end{pmatrix}. \quad (34)$$

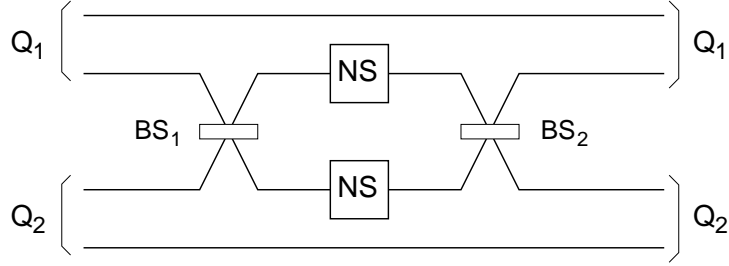


Figure 2. C-Z gate: The implementation of C-Z gate is made by a combination of the nonlinear sign gate and the physics of Hong-Ou-Mandel (HOM) interferometer.

This corresponds to two phase shifters of $e^{i\pi/2}$ in the lower path before and after the ordinary beam splitters. Similarly, for BS_2 we have

$$BS_2 ::= \begin{pmatrix} i & 0 \\ 0 & 1 \end{pmatrix} \begin{pmatrix} \sqrt{\eta_2} & -i\sqrt{1-\eta_2} \\ -i\sqrt{1-\eta_2} & \sqrt{\eta_2} \end{pmatrix} \begin{pmatrix} i & 0 \\ 0 & 1 \end{pmatrix}, \quad (35)$$

which corresponds to two phase shifters of $e^{i\pi/2}$ in the upper path before and after the ordinary beam splitters with the reflection coefficient η_2 .

2.4. Non-deterministic C-Z gate

To make the C-Z gate, all we need is to change the sign of the input when the input is corresponding to $|1\rangle_L|1\rangle_L$ state. Given arbitrary two qubits

$$\begin{aligned} |Q_1\rangle &= \alpha_0|0\rangle_L + \alpha_1|1\rangle_L = \alpha_0|0\rangle_1|1\rangle_2 + \alpha_1|1\rangle_1|0\rangle_2, \\ |Q_2\rangle &= \alpha'_0|0\rangle_L + \alpha'_1|1\rangle_L = \alpha'_0|0\rangle_3|0\rangle_4 + \alpha'_1|1\rangle_3|0\rangle_4, \end{aligned} \quad (36)$$

the transformation by applying a C-Z gate, can be written as

$$\begin{aligned} |Q_1\rangle|Q_2\rangle &\Rightarrow \alpha_0\alpha'_0|0\rangle_L|0\rangle_L + \alpha_0\alpha'_1|0\rangle_L|1\rangle_L + \alpha_1\alpha'_0|1\rangle_L|0\rangle_L - \alpha_1\alpha'_1|1\rangle_L|1\rangle_L \\ &= \alpha_0\alpha'_0|0, 1, 0, 1\rangle + \alpha_0\alpha'_1|0, 1, 1, 0\rangle + \alpha_1\alpha'_0|1, 0, 0, 1\rangle - \alpha_1\alpha'_1|1, 0, 1, 0\rangle. \end{aligned} \quad (37)$$

where the modes 1, 2 are designated for the control qubit, and 3, 4 are for the target qubit, and the number state representation was given in this order (see Fig.2). We can immediately see that when there is a sign change only when there is one photon in mode 1 and one photon in mode 3.

Here the two additional 50/50 beam splitters (shown in the figure) need to be mutually conjugate given by

$$BS_1 = BS(\theta = \pi/2, \phi = -\pi/2) ::= \frac{1}{\sqrt{2}} \begin{pmatrix} 1 & -i \\ -i & 1 \end{pmatrix} \quad (38)$$

$$BS_2 = BS(\theta = \pi/2, \phi = \pi/2) ::= \frac{1}{\sqrt{2}} \begin{pmatrix} 1 & i \\ i & 1 \end{pmatrix} \quad (39)$$

To summarize, we need six asymmetric beam splitters (or six ordinary symmetric beams plitters and six phase shifters), four single-photon detectors, and two mutually conjugate 50/50 beam splitters for the C-Z gate. In

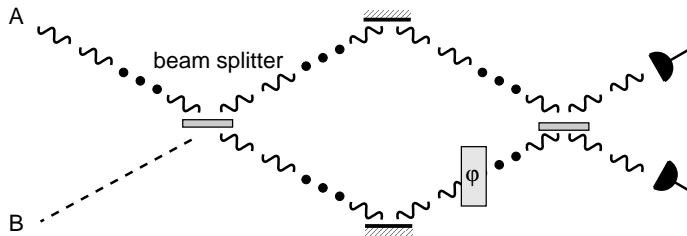


Figure 3. A typical Mach-Zehnder interferometer where the input light is incident on input port A while only vacuum comes into input port B.

addition four polarization beam splitters in order to convert the polarization qubits to the dual-rail qubits back and forth. This is a non-deterministic gate in that the operation is successful only one in sixteen times on average. The probability of success then can be boosted by using gate-teleportation technique and sufficient number of ancilla photons. It has been also demonstrated that such a nondeterministic two-qubit gate can be made for qubits defined by the polarization degree of freedom.^{7,8} Reliable single-photon sources and the ability to discriminate the number of incoming photons play the essential roles in the realization of such nonlinear quantum gates in optical quantum computing.

3. QUANTUM METROLOGY AND IMAGING

In a Mach-Zehnder interferometer, the input light field is divided into two different paths by a beam splitter, and recombined by another beam splitter. The phase difference between the two paths is then measured by balanced detection of the two output modes (see Fig. 3). We may think of the upper and lower paths as the two states in which a single light quanta can occupy. With a coherent laser field as the input the phase sensitivity is given by the shot noise limit $1/\sqrt{N}$, where N is the average number of photons passing through the interferometer during measurement time. When the number of photons is exactly known (i.e., the input is a Fock state $|N\rangle$), the phase sensitivity is still given by $1/\sqrt{N}$, indicating that the photon counting noise does not originate from the intensity fluctuations of the input beam, but rather from the Poissonian “sorting noise” of the beam splitter.

There have been various proposals for achieving Heisenberg-limited sensitivity, depending on the input states and the detection schemes. In particular, the Yurke state approach has the same measurement scheme as the conventional Mach-Zehnder interferometer; a direct detection of the difference current.^{9–12} It is, however, not easy to generate the desired correlation in the input state. On the other hand, the dual Fock-state approach finds a rather simple input state, but requires a complicated data processing methods.^{13,14} However, by a simple utilization of the projective measurements with linear optical devices, it is possible to generate a desired correlation in the Yurke state directly from the dual Fock state.

Let us consider a linear optical setup depicted in Fig.4. For a given dual Fock-state input $|N, N\rangle_{ab}$, the output state conditioned on, for example, a two-fold coincident count is given by

$$\frac{1}{\sqrt{2}} [|N, N-2\rangle + |N-2, N\rangle]. \quad (40)$$

It is not difficult to see that the condition of the coincident detection yields either one of the two modes before the beam splitter must contain two photons while the other modes contains no photon. This is an inverse-HOM situation where one photon at each mode cannot contribute to the coincident detection. Consequently, the coincident detection results in a situation where the main modes a and b can only lose two photons or not at all.

Here the probability success of this event can be optimized by choosing the reflection coefficient of the first beam splitters. For the reflection coefficient of $|r|^2 = 1/N$, its asymptotic value is found as $1/(2e^2)$, independent of N . Furthermore, using a stack of such devices with appropriate phase shifters, we have developed a method for the generation of maximally path-entangled states of the form $|N, 0\rangle_{ab} + |0, N\rangle_{ab}$, the so-called NOON state, with an arbitrary number of photons.¹⁵

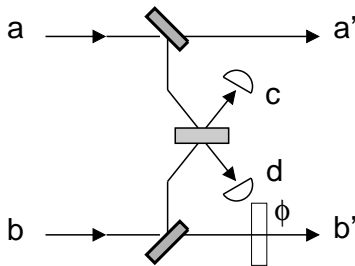


Figure 4. A Yurke-type quantum correlation between the two modes can be produced with a dual Fock-state. Suppose we post-select the outcome, conditioned upon only one photon detection by either one of the two detectors. Due to the 50:50 beam splitter in the midway, it is not possible to tell whether mode a or b lost one photon.

Quantum correlations can also be applied to optical lithography. In recent work it has been shown that the Rayleigh diffraction limit in optical lithography can be circumvented by the use of path-entangled photon number states.¹⁶ The desired N -photon path-entangled state, for N -fold resolution enhancement, is the NOON states.

Consider the simple case of a two-photon Fock state $|1\rangle_A|1\rangle_B$, which is a natural component of a spontaneous parametric down-conversion event. After passing through a 50/50 beam splitter, it becomes an entangled number state of the form $|2\rangle_A|0\rangle_B + |0\rangle_A|2\rangle_B$. Interference suppresses the probability amplitude of $|1\rangle_A|1\rangle_B$. According to quantum mechanics, it is not possible to tell whether both photons took path A or B after the beam splitter.

When parametrizing the position x on the surface by $\varphi = \pi x/\lambda$, the deposition rate of the two photons onto the substrate becomes $1 + \cos 2\varphi$, which has twice better resolution $\lambda/8$ than that of single-photon absorption, $1 + \cos \varphi$, or that of uncorrelated two-photon absorption, $(1 + \cos \varphi)^2$. For the NOON state we obtain the deposition rate $1 + \cos N\varphi$, corresponding to a resolution enhancement of $\lambda/(4N)$.

It is well known that the two-photon NOON state can be generated using a Hong-Ou-Mandel (HOM) interferometer¹⁷ and two single-photon input states. A 50/50 beam splitter, however, is not sufficient for producing path-entangled states with a photon number larger than two.

4. UNIVERSAL NOON STATE GENERATION

As we have mentioned earlier, one of the possible ways to generate a two-mode entangled many-photon state, such as a NOON state, is to make use of an optical nonlinearity. However, due to a relatively small average number of photons involved an overall effect of the nonlinearity is extremely tiny and practically one cannot make use of it. An alternative way to enable an effective photon-photon interaction is to use ancilla modes and projective measurements. In this case a *universal NOON state generating machine* can be built consisting out of two main blocks Fig.5.

The first part is a R -port unitary device producing a linear superposition of the $R - 2$ input ancilla modes and two target input modes. The second part is a non-unitary projection device performing a photodetection of $m_j, j = 2, \dots, R$ photons in each of the output ancilla modes. In this way, an interplay between the number of input photons, parameters of the R -port linear device and the number of detected output ancilla photons determines a state of two output target modes.

In general there is a limitation on a possible size of an output NOON state in such a generating machine. Here we formulate the following “no-go theorem”: Suppose we have an R -port NOON state generating machine as depicted in Fig.5. The NOON state can be generated in the two output modes with at most R photons. In other words, in order to generate a NOON state $|\psi\rangle = \frac{1}{\sqrt{2}}(|N, 0\rangle + |0, N\rangle)$ one requires at least N input modes. It means that the number of the resources needed to build a high-NOON state (a NOON state with high N) grows polynomially in N . However, the success probability drops down exponentially.

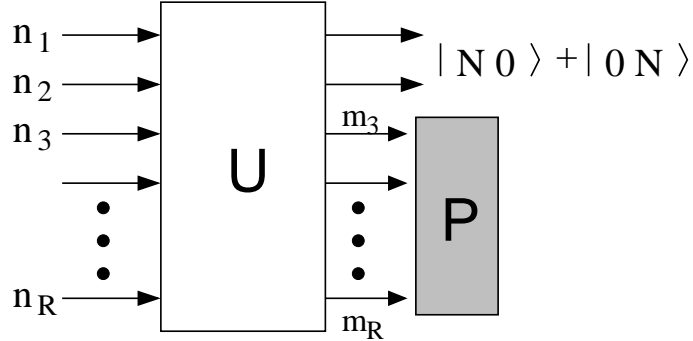


Figure 5. NOON state generating machine. R input modes, fed with $n_i, i = 1, \dots, R$ photons each, are transformed into a linear superposition of the output modes by a unitary operation U . A successive projective measurement P of $m_j, j = 3, \dots, R$ photons in $R - 2$ output modes leads to a collapse of the wave function into a NOON state in the unmeasured output modes 1 and 2.

As an example illustrating our statements we consider a NOON state generator with four input modes, i.e., the number of ancilla modes is 2. According to the theorem formulated above, we can generate at most a four-photon NOON state $|\psi\rangle = \frac{1}{\sqrt{2}}(|4, 0\rangle + |0, 4\rangle)$. This can be done in a number of different ways with different success probabilities. Depending on the availability of the resources and photodetection preferences we can construct different realizations of the NOON state generator.

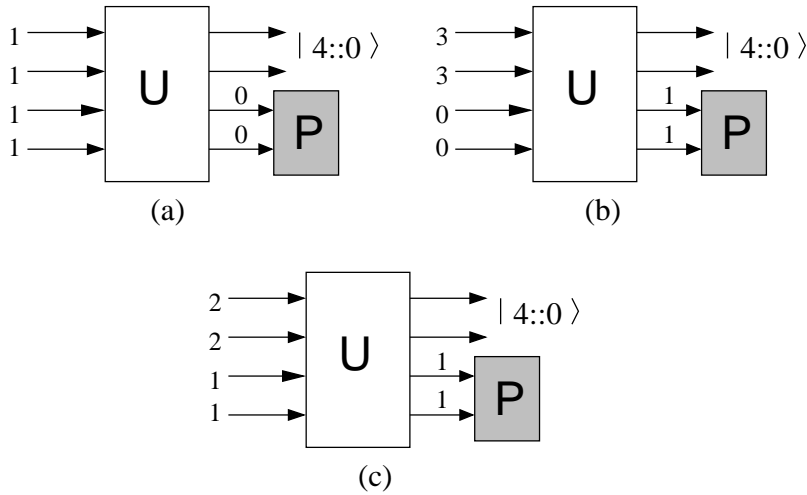


Figure 6. Possible allowed configurations for the four-photon NOON state generation. $|4 :: 0\rangle$ denotes $\frac{1}{\sqrt{2}}(|4, 0\rangle + |0, 4\rangle)$.¹⁵

If one wants, for example, to rely on a vacuum detection (or, in other words, no-photons detection) in both output ancilla modes, then one can realize a scheme depicted on Fig.6(a). In this case each input mode is fed with only one photon and the four-photon NOON state is generated upon a vacuum measurement in both output ancilla modes.¹⁸ Alternatively, a scheme based on a coincidence detection in the output ancilla modes is presented on Fig.6(b). Here, the input ancilla modes contain zero photons.¹⁹ A scheme based on a coincidence detection and non-zero ancilla input is also possible and depicted on Fig.6(c). The variety of possible realizations of a given NOON state sets up a question about the most optimal configuration of a NOON state generator.

REFERENCES

1. D. Bouwmeester, A. Ekert, and A. Zeilinger, *The Physics of Quantum Information: Quantum Cryptography, Quantum Teleportation, and Quantum Computing* (Springer, Berlin, 2000).
2. H. Lee, P. Kok, and J.P. Dowling, “A quantum Rosetta stone for interferometry,” *J. Mod. Opt.* **49**, 2325 (2002).
3. M.O. Scully and M.S. Zubairy, *Quantum Optics* (Cambridge University Press, Cambridge, UK, 1997).
4. G.J. Milburn, *Phys. Rev. Lett.* **62**, 2124 (1989).
5. E. Knill, R. Laflamme, and G.J. Milburn, “A scheme for efficient quantum computation with linear optics,” *Nature* **409**, 46 (2001).
6. T.C. Ralph, A.G. White, W.J. Munro, and G.J. Milburn, “Simple scheme for efficient linear optics quantum gates,” *Phys. Rev. A* **65**, 012314 (2001).
7. T.B. Pittman, B.C. Jacobs, and J.D. Franson, “Probabilistic quantum logic operations using polarizing beam splitters,” *Phys. Rev. A* **64**, 062311 (2001).
8. T.B. Pittman, B.C. Jacobs, and J.D. Franson, “Demonstration of nondeterministic quantum logic operations using linear optical elements,” *Phys. Rev. Lett.* **88**, 257902 (2002).
9. B. Yurke, “Input state for enhancement of fermion interferometer sensitivity,” *Phys. Rev. Lett.* **56**, 1515 (1986).
10. H.P. Yuen, “Generation, Detection and Application of High-Intensity Photon-Number-Eigenstate Fields,” *Phys. Rev. Lett.* **56**, 2176 (1986).
11. B. Yurke, S.L. McCall, and J.R. Klauder, “SU(2) and SU(1,1) interferometers,” *Phys. Rev. A* **33**, 4033 (1986).
12. J.P. Dowling, “Correlated input, matter-wave interferometer: Quantum-noise limits to the atom-laser gyroscope,” *Phys. Rev. A* **57**, 4736 (1998).
13. M.J. Holland and K. Burnett, “Interferometric detection of optical phase shifts at the Heisenberg limit,” *Phys. Rev. Lett.* **71**, 1355 (1993).
14. T. Kim, O. Pfister, M.J. Holland, J. Noh, and J.L. Hall, “Influence of decorrelation on Heisenberg-limited interferometry with quantum correlated photons,” *Phys. Rev. A* **57**, 4004 (1998).
15. P. Kok, H. Lee, and J.P. Dowling, “The creation of large photon-number path entanglement conditioned on photodetection,” *Phys. Rev. A* **65**, 052104 (2002).
16. A.N. Boto *et al.*, “Quantum interferometric optical lithography: Exploiting entanglement to beat the diffraction limit,” *Phys. Rev. Lett.* **85**, 2733 (2000).
17. C.K. Hong, Z.Y. Ou, and L. Mandel, “Measurement of subpicosecond time intervals between two photons by interference,” *Phys. Rev. Lett.* **59**, 2044 (1987).
18. J. Fiurásek, “Conditional generation of N-photon entangled state of light,” *Phys. Rev. A* **65** 053818 (2002).
19. H. Lee, P. Kok, N.J. Cerf, and J.P. Dowling, “Linear optics and projective measurements alone suffice to create large-photon-number path entanglement,” *Phys. Rev. A* **65**, 030101 (R) (2002).